

# Revisiting wrong sign Yukawa coupling of type II two-Higgs-doublet model in light of the recent LHC data

Lei Wang, Hong-Xin Wang, Xiao-Fang Han\*

*Department of Physics, Yantai University, Yantai 264005, China*

## Abstract

In light of the recent LHC Higgs data, we examine the parameter space of type II two-Higgs-doublet model in which the 125 GeV Higgs has the wrong sign Yukawa couplings. Combining related theoretical and experimental limits, we find that the LHC Higgs data exclude most of the parameter space of the wrong sign Yukawa coupling. For  $m_H = 600$  GeV, the allowed samples are mainly distributed in several corners and narrow bands of  $m_A < 20$  GeV,  $30$  GeV  $< m_A < 120$  GeV,  $240$  GeV  $< m_A < 300$  GeV,  $380$  GeV  $< m_A < 430$  GeV, and  $480$  GeV  $< m_A < 550$  GeV. For  $m_A = 600$  GeV,  $m_H$  is required to be less than 470 GeV. The light pseudo-scalar with a mass of 20 GeV is still allowed in case of the wrong sign Yukawa coupling of 125 GeV Higgs.

PACS numbers: 12.60.Fr, 14.80.Ec, 14.80.Bn

---

\*) Corresponding author. Email address: xfhan@ytu.edu.cn (X. Han)

## I. INTRODUCTION

The two-Higgs-doublet model (2HDM) [1] is a popular extension of the SM by introducing another  $SU(2)_L$  Higgs doublet, which contains neutral CP-even Higgs bosons  $h$  and  $H$ , neutral pseudoscalar  $A$ , and charged Higgs  $H^\pm$ . There are four typical 2HDMs in which the flavor changing neutral currents at tree level are absent, namely the type-I [2, 3], the type II [2, 4], the lepton-specific, and the flipped models [5–8]. In the type II model, the Yukawa couplings of leptons and down-type quarks can be enhanced by a factor  $\tan\beta$ . Therefore, the flavor observables and the LHC searching for Higgs can give more strict restrictions to the type II model than the other three models. In the type II 2HDM, the 125 GeV Higgs can have a wrong sign Yukawa coupling besides a SM-like coupling. Compared with the SM, at least one of the Yukawa couplings of the 125 GeV Higgs has an opposite sign to the couplings of gauge bosons, which is extensively studied in Refs. [9–24].

At the beginning of 2017, we used the LHC Higgs data at that time to explore the parameter space of type II 2HDM, and found that the  $H/A \rightarrow \tau^+\tau^-$  and  $A \rightarrow hZ$  modes can give strong restrictions on the parameter space of the wrong sign Yukawa coupling [22]. Very recently, Refs. [23, 24] examined the parameter space with degenerate heavy Higgs masses in the framework of this model. In this work, we will re-examine the wrong sign Yukawa coupling in the type II 2HDM, and scan over the parameter space extensively by considering the recent ATLAS and CMS Higgs data.

Our work is organized as follows. In Sec. II we introduce the type II 2HDM briefly. In Sec. III we implement detailed numerical calculations. In Sec. IV, we display the allowed parameter space by considering the relevant theoretical and experimental restrictions. In Sec. V, we provide our conclusions.

## II. TYPE II TWO-HIGGS-DOUBLET MODEL

The scalar potential with a softly broken discrete  $Z_2$  symmetry is given by [25]

$$\begin{aligned} V = & m_{11}^2(\Phi_1^\dagger\Phi_1) + m_{22}^2(\Phi_2^\dagger\Phi_2) - \left[ m_{12}^2(\Phi_1^\dagger\Phi_2 + \text{h.c.}) \right] \\ & + \frac{\lambda_1}{2}(\Phi_1^\dagger\Phi_1)^2 + \frac{\lambda_2}{2}(\Phi_2^\dagger\Phi_2)^2 + \lambda_3(\Phi_1^\dagger\Phi_1)(\Phi_2^\dagger\Phi_2) + \lambda_4(\Phi_1^\dagger\Phi_2)(\Phi_2^\dagger\Phi_1) \\ & + \left[ \frac{\lambda_5}{2}(\Phi_1^\dagger\Phi_2)^2 + \text{h.c.} \right]. \end{aligned} \tag{1}$$

We focus on the CP-conserving case in which all  $\lambda_i$  and  $m_{12}^2$  are real. The two complex Higgs doublets have the hypercharge  $Y = 1$ :

$$\Phi_1 = \begin{pmatrix} \phi_1^+ \\ \frac{1}{\sqrt{2}}(v_1 + \phi_1^0 + ia_1) \end{pmatrix}, \quad \Phi_2 = \begin{pmatrix} \phi_2^+ \\ \frac{1}{\sqrt{2}}(v_2 + \phi_2^0 + ia_2) \end{pmatrix}. \quad (2)$$

In the above formula,  $v_1$  and  $v_2$  are the electroweak vacuum expectation values (VEVs) with  $v^2 = v_1^2 + v_2^2 = (246 \text{ GeV})^2$  and  $\tan \beta = v_2/v_1$ . After the spontaneous electroweak symmetry is broken, we get five physical Higgs particles, two neutral CP-even  $h$  and  $H$ , one neutral pseudoscalar  $A$ , and a pair of charged scalars  $H^\pm$ .

The Yukawa interactions can be given as

$$-\mathcal{L} = Y_{u2} \bar{Q}_L \tilde{\Phi}_2 u_R + Y_{d1} \bar{Q}_L \Phi_1 d_R + Y_{\ell 1} \bar{L}_L \Phi_1 e_R + \text{h.c.}, \quad (3)$$

in which  $Q_L^T = (u_L, d_L)$ ,  $L_L^T = (\nu_L, l_L)$ , and  $\tilde{\Phi}_{1,2} = i\tau_2 \Phi_{1,2}^*$ .  $Y_{u2}$ ,  $Y_{d1}$  and  $Y_{\ell 1}$  are  $3 \times 3$  matrices.

The neutral Higgs Yukawa couplings normalized to the SM are as follows.

$$\begin{aligned} y_h^{f_i} &= [\sin(\beta - \alpha) + \cos(\beta - \alpha)\kappa_f], \\ y_H^{f_i} &= [\cos(\beta - \alpha) - \sin(\beta - \alpha)\kappa_f], \\ y_A^{f_i} &= -i\kappa_f \text{ (for u)}, \quad y_A^{f_i} = i\kappa_f \text{ (for d, } \ell), \\ &\text{with } \kappa_d = \kappa_\ell \equiv -\tan \beta, \quad \kappa_u \equiv 1/\tan \beta. \end{aligned} \quad (4)$$

The Yukawa interactions of the charged Higgs are given as,

$$\mathcal{L}_Y = -\frac{\sqrt{2}}{v} H^+ \left\{ \bar{u}_i [\kappa_d (V_{CKM})_{ij} m_{dj} P_R - \kappa_u m_{ui} (V_{CKM})_{ij} P_L] d_j + \kappa_\ell \bar{\nu} m_\ell P_R \ell \right\} + \text{h.c.}, \quad (5)$$

in which  $i, j = 1, 2, 3$ .

The neutral Higgs couplings with gauge bosons normalized to the SM are

$$y_h^V = \sin(\beta - \alpha), \quad y_H^V = \cos(\beta - \alpha), \quad (6)$$

with  $V$  denoting  $W$  or  $Z$ .

In type II 2HDM, the SM-like Higgs has not only the SM-like coupling but also the wrong sign Yukawa coupling,

$$\begin{aligned} y_h^{f_i} \times y_h^V &> 0 \text{ for SM-like coupling,} \\ y_h^{f_i} \times y_h^V &< 0 \text{ for wrong sign Yukawa coupling.} \end{aligned} \quad (7)$$

In case of the SM-like coupling, the 125 GeV Higgs couplings are very close to those in the SM, which has an alignment limit. Now we introduce the wrong sign Yukawa coupling. The absolute values of  $y_h^{f_i}$  and  $y_h^V$  should be close to 1.0 because of the restrictions of 125 GeV Higgs signal data. So we obtain

$$\begin{aligned} y_h^{f_i} &= -1 + \epsilon, \quad y_h^V \simeq 1 - 0.5 \cos^2(\beta - \alpha) \quad \text{for } \sin(\beta - \alpha) > 0 \text{ and } \cos(\beta - \alpha) > 0, \\ y_h^{f_i} &= 1 - \epsilon, \quad y_h^V \simeq -1 + 0.5 \cos^2(\beta - \alpha) \quad \text{for } \sin(\beta - \alpha) < 0 \text{ and } \cos(\beta - \alpha) > 0. \end{aligned} \quad (8)$$

Here  $|\epsilon|$  and  $|\cos(\beta - \alpha)|$  are much less than 1. From Eq. (4), we can get

$$\begin{aligned} \kappa_f &= \frac{-2 + \epsilon + 0.5 \cos(\beta - \alpha)^2}{\cos(\beta - \alpha)} \ll -1 \quad \text{for } \sin(\beta - \alpha) > 0 \text{ and } \cos(\beta - \alpha) > 0, \\ \kappa_f &= \frac{2 - \epsilon - 0.5 \cos(\beta - \alpha)^2}{\cos(\beta - \alpha)} \gg 1 \quad \text{for } \sin(\beta - \alpha) < 0 \text{ and } \cos(\beta - \alpha) > 0. \end{aligned} \quad (9)$$

In type II 2HDM, the constraints of  $B$ -meson and  $R_b$  require  $\tan\beta$  to be greater than 1, which leads to  $\kappa_d < -1$ ,  $\kappa_\ell < -1$ , and  $0 < \kappa_u < 1$ . Therefore, there is no wrong sign Yukawa coupling for the up-type quark and may exist wrong sign Yukawa couplings of the down-type quark and lepton for  $\sin(\beta - \alpha) > 0$  and  $\cos(\beta - \alpha) > 0$ . Because of the factor "-2" in the numerator in Eq. (9),  $\cos(\beta - \alpha)$  and  $\tan\beta$  in the wrong sign Yukawa coupling region are greater than those in the SM-like coupling region.

### III. NUMERICAL CALCULATIONS

We choose the light CP-even Higgs boson  $h$  as the SM-like Higgs with the mass of 125 GeV. The branching ratio of  $b \rightarrow s\gamma$  gives stringent restrictions on the charged Higgs mass of the type II 2HDM, which requires  $m_{H^\pm} > 570$  GeV [26].

In the calculation, we take account of the following constraints and observables:

- (1) The electroweak precision data and theoretical constraints. We use the 2HDMC [27] to consider the theoretical constraints from the vacuum stability, unitarity and perturbativity, and calculate the oblique parameters ( $S$ ,  $T$ ,  $U$ ). We take the recent fit results for  $S$ ,  $T$ ,  $U$  in Ref. [28],

$$S = 0.02 \pm 0.10, \quad T = 0.07 \pm 0.12, \quad U = 0.00 \pm 0.09, \quad (10)$$

with correlation coefficients,

$$\rho_{ST} = 0.89, \quad \rho_{SU} = -0.54, \quad \rho_{TU} = -0.83. \quad (11)$$

- (2) The heavy-flavor observables and  $R_b$  constraints. We use **SuperIso-3.4** [29] to calculate the branching ratio of  $B \rightarrow X_s \gamma$ .  $\Delta m_{B_s}$  is calculated following the formulas of Ref. [30]. Furthermore, we consider the  $R_b$  constraints of bottom quarks in  $Z$  decays, which is calculated following the formulas of Refs. [31, 32]. Recently, the  $R_b$  observable is also considered in some works on the 2HDM [33, 34]
- (3) The 125 GeV Higgs signal data. We use the version 2.0 of **Lilith** [35] to perform the calculation of  $\chi^2$  for the 125 GeV Higgs signal data combining the LHC run-I and run-II data (up to datasets of  $36 \text{ fb}^{-1}$ ). We are particularly concerned with the surviving samples for  $\chi^2 - \chi_{\min}^2 \leq 6.18$ , in which  $\chi_{\min}^2$  is the minimum of  $\chi^2$ . These samples are within the  $2\sigma$  range in two-dimensional plane of model parameters.

- (4) The LHC searching for additional Higgs bosons. We use the **HiggsBounds-4.3.1** [36, 37] to perform the exclusion limits from the Higgs searches at LEP at 95% confidence level.

At the LHC run-I and run-II, the ATLAS and CMS have searched the additional Higgs via its decaying into various SM modes and some exotic channels. Because of the destructive interference contributions to  $gg \rightarrow A$  production which come from the top-quark loop and the bottom-quark loop in the type II 2HDM, the cross section decreases with the increasing  $\tan\beta$ , and reaches a minimum value for a moderate  $\tan\beta$ , which is dominated by the bottom-quark loop for a large enough value of  $\tan\beta$ . The cross section of  $gg \rightarrow H$  production not only depends on  $\tan\beta$  and  $m_H$ , but also  $\sin(\beta - \alpha)$ . We calculate the cross sections for  $A$  and  $H$  in the gluon fusion and  $b\bar{b}$ -associated production at NNLO in QCD via **SusHi** [38]. The cross sections of  $H$  via vector boson fusion process is derived from the data at LHC Higgs Cross Section Working Group [39]. We use the **2HDMC** to calculate the branching ratios of various decay channels of  $A$  and  $H$ . In Table I and Table II, we show a complete list of the additional Higgs searches considered in this paper. When  $1 \leq \tan\beta \leq 30$ , the heavy charged scalar searches at LHC cannot impose restrictions on the model for  $m_{H^\pm} > 500 \text{ GeV}$  [40]. So we do not include the heavy charged Higgs searches.

For the  $A \rightarrow hZ$  channel, the CMS collaboration also presented result of  $h \rightarrow \tau^+ \tau^-$  at the 13 TeV LHC with an integrated luminosity of  $35.9 \text{ fb}^{-1}$  in Ref. [78]. However, compared to the results of Refs. [71, 72], the decay width  $\Gamma_A/m_A$  corresponding to the

Channel	Experiment [TeV]	Mass range [GeV]	Luminosity [fb <sup>-1</sup> ]
$gg/b\bar{b} \rightarrow H/A \rightarrow \tau^+\tau^-$	ATLAS 8 [41]	90-1000	19.5-20.3
$gg/b\bar{b} \rightarrow H/A \rightarrow \tau^+\tau^-$	CMS 8 [42]	90-1000	19.7
$gg/b\bar{b} \rightarrow H/A \rightarrow \tau^+\tau^-$	ATLAS 13 [43]	200-1200	13.3
$gg/b\bar{b} \rightarrow H/A \rightarrow \tau^+\tau^-$	CMS 13 [44]	90-3200	12.9
$gg \rightarrow H/A \rightarrow \tau^+\tau^-$	CMS 13 [45]	200-2250	36.1
$b\bar{b} \rightarrow H/A \rightarrow \tau^+\tau^-$	CMS 13 [45]	200-2250	36.1
$b\bar{b} \rightarrow H/A \rightarrow \tau^+\tau^-$	CMS 8 [46]	25-80	19.7
$b\bar{b} \rightarrow H/A \rightarrow \mu^+\mu^-$	CMS 8 [47]	25-60	19.7
$pp \rightarrow H/A \rightarrow \gamma\gamma$	ATLAS 13 [48]	200-2400	15.4
$gg \rightarrow H/A \rightarrow \gamma\gamma$	CMS 8+13 [49]	500-4000	12.9
$gg \rightarrow H/A \rightarrow \gamma\gamma + t\bar{t}H/A (H/A \rightarrow \gamma\gamma)$	CMS 8 [50]	80-110	19.7
$gg \rightarrow H/A \rightarrow \gamma\gamma + t\bar{t}H/A (H/A \rightarrow \gamma\gamma)$	CMS 13 [50]	70-110	35.9
$VV \rightarrow H \rightarrow \gamma\gamma + VH (H \rightarrow \gamma\gamma)$	CMS 8 [50]	80-110	19.7
$VV \rightarrow H \rightarrow \gamma\gamma + VH (H \rightarrow \gamma\gamma)$	CMS 13 [50]	70-110	35.9
$gg/VV \rightarrow H \rightarrow W^+W^-$	ATLAS 8 [51]	300-1500	20.3
$gg/VV \rightarrow H \rightarrow W^+W^- (\ell\nu\ell\nu)$	ATLAS 13 [52]	300-3000	13.2
$gg \rightarrow H \rightarrow W^+W^- (\ell\nu qq)$	ATLAS 13 [53]	500-3000	13.2
$gg/VV \rightarrow H \rightarrow W^+W^- (\ell\nu qq)$	ATLAS 13 [54]	200-3000	36.1
$gg/VV \rightarrow H \rightarrow W^+W^- (e\nu\mu\nu)$	ATLAS 13 [55]	200-3000	36.1
$gg/VV \rightarrow H \rightarrow ZZ$	ATLAS 8 [56]	160-1000	20.3
$gg \rightarrow H \rightarrow ZZ(\ell\nu\nu)$	ATLAS 13 [57]	300-1000	13.3
$gg \rightarrow H \rightarrow ZZ(\nu\nu qq)$	ATLAS 13 [58]	300-3000	13.2
$gg/VV \rightarrow H \rightarrow ZZ(\ell qq)$	ATLAS 13 [58]	300-3000	13.2
$gg/VV \rightarrow H \rightarrow ZZ(\ell\ell\ell)$	ATLAS 13 [59]	200-3000	14.8
$gg/VV \rightarrow H \rightarrow ZZ(\ell\ell\ell + \ell\nu\nu)$	ATLAS 13 [60]	200-2000	36.1
$gg/VV \rightarrow H \rightarrow ZZ(\nu\nu qq + \ell qq)$	ATLAS 13 [61]	300-5000	36.1

TABLE I: The upper bounds on the production cross-section times the branching ratio of  $\tau^+\tau^-$ ,  $\mu^+\mu^-$ ,  $\gamma\gamma$ ,  $WW$ , and  $ZZ$  for the  $H$  and  $A$  searches at 95% C.L..

Channel	Experiment [TeV]	Mass range [GeV]	Luminosity [ $\text{fb}^{-1}$ ]
$gg \rightarrow H \rightarrow hh \rightarrow (\gamma\gamma)(b\bar{b})$	CMS 8 [62]	250-1100	19.7
$gg \rightarrow H \rightarrow hh \rightarrow (b\bar{b})(b\bar{b})$	CMS 8 [63]	270-1100	17.9
$gg \rightarrow H \rightarrow hh \rightarrow (b\bar{b})(\tau^+\tau^-)$	CMS 8 [64]	260-350	19.7
$gg \rightarrow H \rightarrow hh \rightarrow b\bar{b}b\bar{b}$	ATLAS 13 [65]	300-3000	13.3
$gg \rightarrow H \rightarrow hh \rightarrow b\bar{b}b\bar{b}$	CMS 13 [66]	750-3000	35.9
$gg \rightarrow H \rightarrow hh \rightarrow (b\bar{b})(\tau^+\tau^-)$	CMS 13 [67]	250-900	35.9
$pp \rightarrow H \rightarrow hh$	CMS 13 [68]	250-3000	35.9
$gg \rightarrow A \rightarrow hZ \rightarrow (\tau^+\tau^-)(\ell\ell)$	CMS 8 [64]	220-350	19.7
$gg \rightarrow A \rightarrow hZ \rightarrow (b\bar{b})(\ell\ell)$	CMS 8 [69]	225-600	19.7
$gg \rightarrow A \rightarrow hZ \rightarrow (\tau^+\tau^-)Z$	ATLAS 8 [70]	220-1000	20.3
$gg \rightarrow A \rightarrow hZ \rightarrow (b\bar{b})Z$	ATLAS 8 [70]	220-1000	20.3
$gg/b\bar{b} \rightarrow A \rightarrow hZ \rightarrow (b\bar{b})Z$	ATLAS 13 [71]	200-2000	36.1
$gg/b\bar{b} \rightarrow A \rightarrow hZ \rightarrow (b\bar{b})Z$	CMS 13 [72]	225-1000	35.9
$gg \rightarrow h \rightarrow AA \rightarrow \tau^+\tau^-\tau^+\tau^-$	ATLAS 8 [73]	4-50	20.3
$pp \rightarrow h \rightarrow AA \rightarrow \tau^+\tau^-\tau^+\tau^-$	CMS 8 [74]	5-15	19.7
$pp \rightarrow h \rightarrow AA \rightarrow (\mu^+\mu^-)(b\bar{b})$	CMS 8 [74]	25-62.5	19.7
$pp \rightarrow h \rightarrow AA \rightarrow (\mu^+\mu^-)(\tau^+\tau^-)$	CMS 8 [74]	15-62.5	19.7
$pp \rightarrow h \rightarrow AA \rightarrow (b\bar{b})(\tau^+\tau^-)$	CMS 13 [75]	15-60	35.9
$pp \rightarrow h \rightarrow AA \rightarrow \tau^+\tau^-\tau^+\tau^-$	CMS 13 [76]	4-15	35.9
$gg \rightarrow A(H) \rightarrow H(A)Z \rightarrow (b\bar{b})(\ell\ell)$	CMS 8 [77]	40-1000	19.8
$gg \rightarrow A(H) \rightarrow H(A)Z \rightarrow (\tau^+\tau^-)(\ell\ell)$	CMS 8 [77]	20-1000	19.8

TABLE II: The upper bounds on the production cross-section times the branching ratio for the channels of Higgs-pair and a Higgs production in association with  $Z$  at 95% C.L..

bound of Ref. [78] is not given clearly. Therefore, we do not include the experimental bound of  $A \rightarrow hZ \rightarrow (\tau^+\tau^-)Z$  channel from Ref. [78].

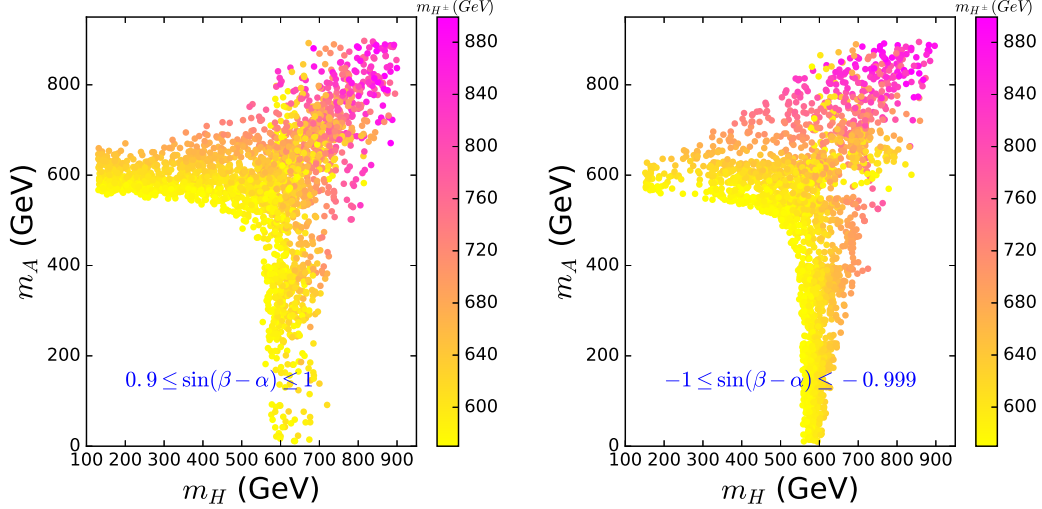


FIG. 1: Scatter plots of  $m_A$  and  $m_H$  satisfying the constraints of vacuum stability, unitarity, perturbativity, and oblique parameters for  $570 \text{ GeV} \leq m_{H^\pm} \leq 900 \text{ GeV}$ .

## IV. RESULTS AND DISCUSSIONS

### A. The constraints from the oblique parameters and the 125 GeV Higgs signal data

In Fig. 1, we display the allowed  $m_A$  and  $m_H$  under the constraints of theory and oblique parameters. Since the branching fraction of  $b \rightarrow s\gamma$  imposes a lower bound on the mass of  $H^\pm$ ,  $m_{H^\pm} > 570 \text{ GeV}$  [26], we take  $570 \text{ GeV} \leq m_{H^\pm} \leq 900 \text{ GeV}$ . When one of  $m_A$  and  $m_H$  is very closed to  $m_{H^\pm}$ , the contributions of 2HDM to the oblique parameters are sizably suppressed, and the other is allowed to have a large mass splitting with  $m_{H^\pm}$ . Therefore, as shown in Fig. 1, it is unfeasible that both  $m_A$  and  $m_H$  are less than 480 GeV, and at least one of  $A$  and  $H$  is required to have a greater mass. When one of  $m_A$  and  $m_H$  is about 600 GeV, the other may have a large mass range, especially for a low mass. However, when  $m_H$  is much greater than 600 GeV and even  $m_H = m_{H^\pm}$ ,  $m_A$  cannot be very small. The main reason is from the requirements of vacuum stability,

$$\lambda_1 > 0, \quad \lambda_2 > 0, \quad \lambda_3 > -\sqrt{\lambda_1\lambda_2}, \quad \lambda_3 + \lambda_4 - |\lambda_5| > -\sqrt{\lambda_1\lambda_2}. \quad (12)$$

To better understand the point, we simply assume a very small  $\cos(\beta - \alpha)$ , and obtain



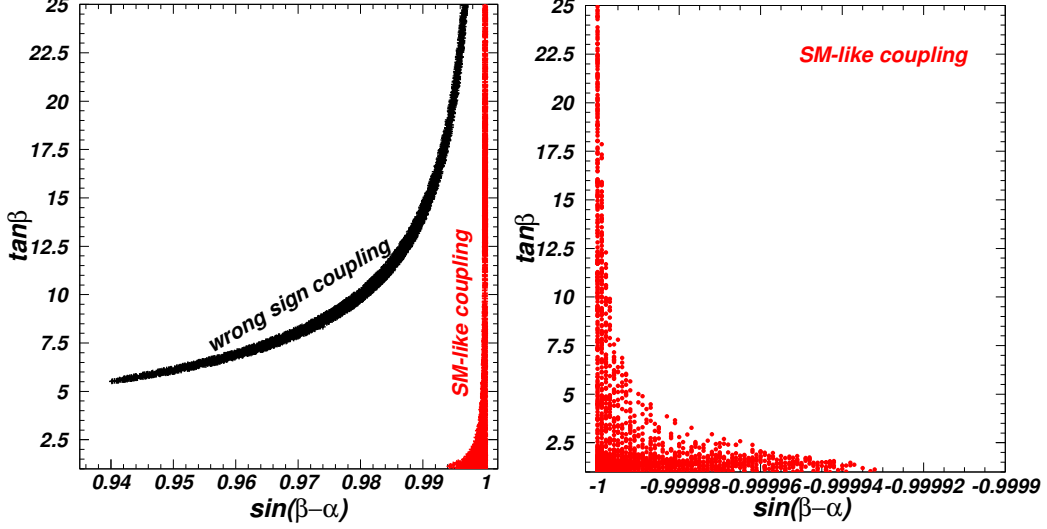


FIG. 2: Scatter plots of  $\sin(\beta-\alpha)$  and  $\tan\beta$  satisfying the constraints of theory, oblique parameters, and the 125 GeV Higgs signal data.

the following relations [18],

$$\begin{aligned}
v^2\lambda_1 &= m_h^2 - \frac{t_\beta (m_{12}^2 - m_H^2 s_\beta c_\beta)}{c_\beta^2}, \\
v^2\lambda_2 &= m_h^2 - \frac{(m_{12}^2 - m_H^2 s_\beta c_\beta)}{t_\beta s_\beta^2}, \\
v^2\lambda_3 &= m_h^2 + 2m_{H^\pm}^2 - 2m_H^2 - \frac{(m_{12}^2 - m_H^2 s_\beta c_\beta)}{s_\beta c_\beta}, \\
v^2\lambda_4 &= m_A^2 - 2m_{H^\pm}^2 + m_H^2 + \frac{(m_{12}^2 - m_H^2 s_\beta c_\beta)}{s_\beta c_\beta}, \\
v^2\lambda_5 &= m_H^2 - m_A^2 + \frac{(m_{12}^2 - m_H^2 s_\beta c_\beta)}{s_\beta c_\beta},
\end{aligned} \tag{13}$$

with  $t_\beta \equiv \tan\beta$ ,  $s_\beta \equiv \sin\beta$ , and  $c_\beta \equiv \cos\beta$ . The first two requirements in Eq. (12) are simultaneously satisfied for  $m_{12}^2 - m_H^2 s_\beta c_\beta \rightarrow 0$ , and the last two are respectively satisfied for

$$m_h^2 + m_{H^\pm}^2 - m_H^2 > 0, \quad m_h^2 + m_A^2 - m_H^2 > 0. \tag{14}$$

The right relation of Eq. (14) implies that  $m_A$  could not be very small for a very large  $m_H$ . The Eq. (14) is obtained in the two limits,  $\cos(\beta - \alpha) \rightarrow 0$  and  $m_{12}^2 - m_H^2 s_\beta c_\beta \rightarrow 0$ . In this paper, we perform exact numerical calculation on the requirements of vacuum stability. The bounds of Eq. (14) can be appropriately loosened by tuning  $\cos(\beta - \alpha)$ ,  $t_\beta$ , and  $m_{12}^2$ .

Using the survival samples in Fig. 1 and imposing the restrictions of the 125 GeV Higgs

signal data, we obtain the scatter plots of  $\tan\beta$  and  $\sin(\beta - \alpha)$  in Fig. 2. From Fig. 2, we see that the 125 GeV Higgs data can give very stringent constraints on  $\tan\beta$  and  $\sin(\beta - \alpha)$ . As discussed above, the Yukawa coupling with wrong sign can be achieved only for  $\sin(\beta - \alpha) > 0$ . In the left panel of Fig. 2,  $\tan\beta$  and  $\sin(\beta - \alpha)$  are respectively required to be larger than 5.0 and as low as 0.94 in case of wrong sign coupling. When the SM-like coupling is applied,  $\sin(\beta - \alpha)$  is restricted to exist in two very narrow bands of  $0.994 \sim 1.0$  and  $-1.0 \sim -0.99993$ , which can be seen in the left and right panels of Fig. 2. For a given  $\sin(\beta - \alpha)$ ,  $\tan\beta$  is imposed a lower limit in case of the Yukawa coupling with wrong sign, and it is required to be as low as 1.0 in case of the SM-like Higgs coupling.

In order to explicitly show the dependence of  $m_A$  ( $m_H$ ) on the other parameters and the specific excluded parameter space from each channel, we do not scan over  $m_A$  and  $m_H$  simultaneously. In the following discussions, considering the allowed Higgs mass spectrum shown in Fig. 1, we will respectively set  $m_A$  or  $m_H$  as 600 GeV, and the other can have a wide mass range, especially for the low mass. Since heavy Higgs can avoid the restrictions of the LHC direct searches easily, the Higgs with a moderate and low mass is more interesting. We scan the parameters for wrong sign Yukawa coupling in the following two scenarios:

$$\begin{aligned}
& 0.93 \leq \sin(\beta - \alpha) \leq 1.0, \quad 1 \leq \tan\beta \leq 25, \quad 570 \text{ GeV} \leq m_{H^\pm} \leq 900 \text{ GeV}, \\
& \text{scenario A : } m_H = 600 \text{ GeV}, \quad 10 \text{ GeV} \leq m_A \leq 900 \text{ GeV}, \\
& \text{scenario B : } m_A = 600 \text{ GeV}, \quad 150 \text{ GeV} \leq m_H \leq 900 \text{ GeV}.
\end{aligned} \tag{15}$$

The free parameter  $m_{12}^2$  is adjusted to satisfy the theoretical constraint. Here we take the conventional method [27],  $0 \leq \beta \leq \frac{\pi}{2}$  and  $-\frac{\pi}{2} \leq \beta - \alpha \leq \frac{\pi}{2}$ . Namely,  $0 \leq \cos(\beta - \alpha) \leq 1$  and  $-1 \leq \sin(\beta - \alpha) \leq 1$ .

## B. Constraints on scenario A

Now we extract the allowed parameter space of scenario A after considering the jointly constraints from pre-LHC (namely the theoretical constraints, electroweak precision data, the flavor observables,  $R_b$ , and the exclusions from searches for Higgs at LEP), the 125 GeV Higgs signal data, and the searches for additional Higgses at the LHC. The surviving samples are projected on the planes of  $m_A$  versus  $\tan\beta$  and  $m_A$  versus  $\sin(\beta - \alpha)$  in Fig. 3. In case of wrong sign Yukawa coupling, the restrictions mentioned above require  $\tan\beta > 5$ .

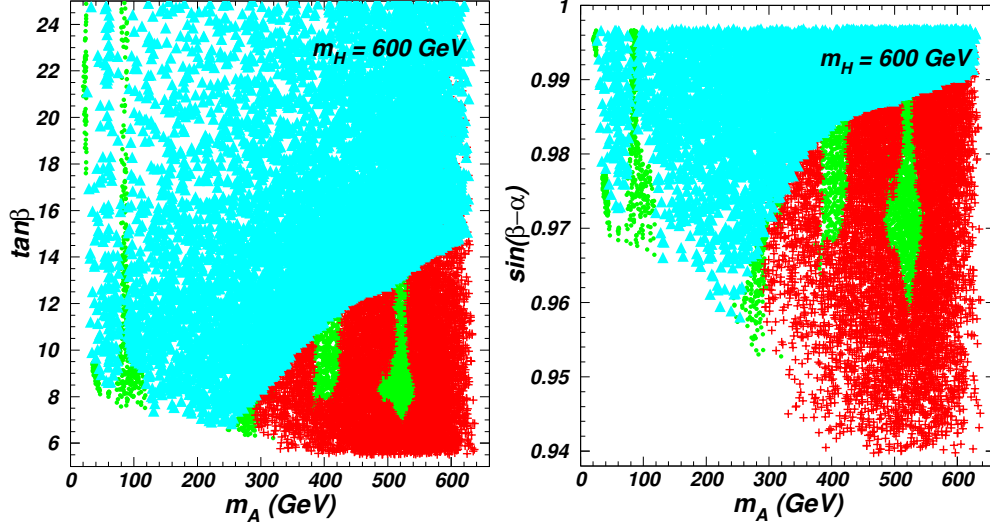


FIG. 3: Scatter plots of  $m_A$  versus  $\tan \beta$  and  $m_A$  versus  $\sin(\beta - \alpha)$  satisfying the constraints of pre-LHC and the 125 GeV Higgs signal data. The triangles (sky blue) and pluses (red) are respectively excluded by the  $A/H \rightarrow \tau^+\tau^-$  and  $A \rightarrow hZ$  channels at the LHC. The bullets (green) are allowed by various LHC direct searches.

For such range of  $\tan \beta$ , the cross section of scalar  $A$  in the gluon fusion production is sizably suppressed, and all the samples are favored by the  $A \rightarrow \gamma\gamma$  and  $A \rightarrow HZ$  modes. Since the 125 GeV Higgs signal data give very strict restrictions on the branching ratio of  $h \rightarrow AA$ , the LHC searching for  $h \rightarrow AA$  cannot impose constraint on the parameter space.

The  $b\bar{b} \rightarrow A \rightarrow \tau^+\tau^-$  channel excludes most of the parameter space for large  $\tan \beta$  and  $gg/b\bar{b} \rightarrow A \rightarrow hZ$  for small  $\tan \beta$ . Because the coupling of  $AhZ$  is proportional to  $\cos(\beta - \alpha)$ , the  $A \rightarrow hZ$  channel tends to exclude the samples with small  $|\sin(\beta - \alpha)|$ . The allowed samples are mainly distributed in several corners and narrow bands. As shown in Table I, the experimental bound of  $A \rightarrow \tau^+\tau^-$  channel is absent for  $m_A < 20$  GeV and  $80 \text{ GeV} < m_A < 90$  GeV, and therefore  $m_A$  in such mass ranges are allowed. In addition, most samples with  $m_A$  in the ranges of  $30 \sim 120$  GeV,  $240 \sim 300$  GeV,  $380 \sim 430$  GeV, and  $480 \sim 550$  GeV are allowed for appropriate  $\tan \beta$  and  $\sin(\beta - \alpha)$ . For the last two bands, the experimental bounds of  $A \rightarrow hZ$  [72] are larger than those of neighbouring mass ranges. Therefore, in the regions of  $380 \text{ GeV} \leq m_A \leq 430 \text{ GeV}$  and  $480 \text{ GeV} \leq m_A \leq 550 \text{ GeV}$ , many samples with large  $\sin(\beta - \alpha)$  can accommodate the bound of  $A \rightarrow hZ$  channel.

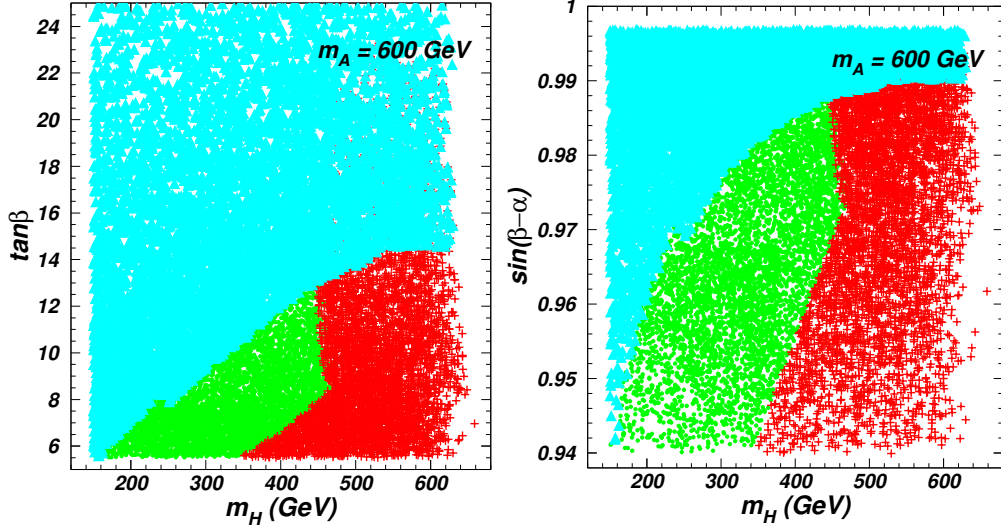


FIG. 4: Scatter plots of  $m_H$  versus  $\tan\beta$  and  $m_H$  versus  $\sin(\beta - \alpha)$  satisfying the constraints of pre-LHC and the 125 GeV Higgs signal data. The triangles (sky blue) and pluses (red) are excluded by the  $H/A \rightarrow \tau^+\tau^-$  and  $A \rightarrow hZ$  channels at the LHC respectively. The bullets (green) are allowed by various LHC direct searches.

### C. Constraints on scenario B

Here we will study the allowed parameter space in scenario B when imposing the jointly restrictions (1)-(4) in Section III. The surviving samples can be seen in the scatter plots of  $m_H$  versus  $\tan\beta$  and  $\sin(\beta - \alpha)$  in Fig. 4. Similar to the discussion in scenario A, the pre-LHC and 125 GeV Higgs signal data require  $\tan\beta > 5$ , and all samples are favored by the  $H \rightarrow VV$ ,  $\gamma\gamma$ ,  $hh$  and  $A \rightarrow HZ$  channels.

Fixing  $m_A = 600$  GeV, the channel  $b\bar{b} \rightarrow H \rightarrow \tau^+\tau^-$  can give upper bounds on  $\tan\beta$  and  $\sin(\beta - \alpha)$ . For instance,  $\tan\beta < 7.0$  (9.2, 14.4) and  $\sin(\beta - \alpha) < 0.96$  (0.98, 0.99) for  $m_H = 200$  GeV (300 GeV, 600 GeV). All samples for  $m_H < 350$  GeV can accommodate the constraints from the channel  $A \rightarrow hZ$ . For such  $m_H$ , the mode  $A \rightarrow HZ$  can increase the total width of  $A$ , and suppress the branching ratio of  $A \rightarrow hZ$  sizably. The channels  $A \rightarrow \tau^+\tau^-$  and  $A \rightarrow hZ$  exclude all the samples for  $m_H > 470$  GeV, and some samples for  $150 \text{ GeV} < m_H < 470 \text{ GeV}$  survive for appropriate  $\tan\beta$  and  $\sin(\beta - \alpha)$ .

Compared with the results of Ref. [22], the recent LHC Higgs data reduce the parameter space sizably. For  $m_H = 600$  GeV, the whole range of  $m_A < 700$  GeV is allowed in Ref. [22], while  $m_A$  is only allowed to vary in several ranges in this paper,  $m_A < 20$  GeV, 30 GeV

$< m_A < 120$  GeV,  $240$  GeV  $< m_A < 300$  GeV,  $380$  GeV  $< m_A < 430$  GeV, and  $480$  GeV  $< m_A < 550$  GeV. For  $m_A = 600$  GeV, the whole range of  $m_H < 700$  GeV is allowed in Ref. [22], while  $m_H < 470$  GeV is required in the paper. Such differences are mainly caused by the experimental data of  $gg/b\bar{b} \rightarrow A \rightarrow hZ$  from Refs. [71, 72], which are not included in Ref. [22].

## V. CONCLUSION

We have studied the status of wrong sign Yukawa coupling of type II 2HDM in light of recent LHC Higgs data, and obtained some interesting conclusions. The channels  $b\bar{b} \rightarrow A/H \rightarrow \tau^+\tau^-$  and  $gg/b\bar{b} \rightarrow A \rightarrow hZ$  exclude most of the parameter space for large  $\tan\beta$  and small  $\tan\beta$ , respectively. For  $m_H = 600$  GeV, the allowed samples are mainly distributed in several corners and narrow bands of  $m_A < 20$  GeV,  $30$  GeV  $< m_A < 120$  GeV,  $240$  GeV  $< m_A < 300$  GeV,  $380$  GeV  $< m_A < 430$  GeV, and  $480$  GeV  $< m_A < 550$  GeV. For  $m_A = 600$  GeV,  $m_H$  is required to be less than 470 GeV.

### Acknowledgment

This work was supported by the National Natural Science Foundation of China under grant 11975013, by the Natural Science Foundation of Shandong province (ZR2017JL002 and ZR2017MA004).

- 
- [1] T. D. Lee, Phys. Rev. D **8**, 1226 (1973).
  - [2] H. E. Haber, G. L. Kane and T. Sterling, Nucl. Phys. B **161**, 493 (1979).
  - [3] L. J. Hall and M. B. Wise, Nucl. Phys. B **187**, 397 (1981).
  - [4] J. F. Donoghue and L. F. Li, Phys. Rev. D **19**, 945 (1979).
  - [5] V. D. Barger, J. L. Hewett and R. J. N. Phillips, Phys. Rev. D **41**, 3421 (1990).
  - [6] Y. Grossman, Nucl. Phys. B **426**, 3 (1994).
  - [7] A. G. Akeroyd and W. J. Stirling, Nucl. Phys. B **447**, 3 (1995).
  - [8] A. G. Akeroyd, Phys. Lett. B **377**, 95 (1996).
  - [9] I. F. Ginzburg, M. Krawczyk, P. Osland, arXiv:hep-ph/0101208.

- [10] P. M. Ferreira, J. F. Gunion, H. E. Haber and R. Santos, Phys. Rev. D **89**, 115003 (2014).
- [11] B. Dumont, J. F. Gunion, Y. Jiang and S. Kraml, Phys. Rev. D **90**, 035021 (2014).
- [12] D. Fontes, J. C. Romão and J. P. Silva, Phys. Rev. D **90**, 015021 (2014).
- [13] P. M. Ferreira, J. F. Gunion, H. E. Haber, R. Santos, Phys. Rev. D **89**, 115003 (2014).
- [14] D. Fontes, J. C. Romao, J. P. Silva, Phys. Rev. D **90**, 015021 (2014).
- [15] P. M. Ferreira, R. Guedes, M. O. P. Sampaio, R. Santos, JHEP **1412**, 067 (2014).
- [16] L. Wang, X.-F. Han, JHEP **1505**, 039 (2015).
- [17] G. C. Dorsch, S. J. Huber, K. Mimasu, J. M. No, Phys. Rev. D **93**, 115033 (2016).
- [18] F. Kling, J. M. No, S. Su, JHEP **1609**, 093 (2016).
- [19] A. Biswas, A. Lahiri, Phys. Rev. D **93**, 115017 (2016).
- [20] T. Modak, J. C. Romao, S. Sadhukhan, J. P. Silva, R. Srivastava, Phys. Rev. D **94**, 075017 (2016).
- [21] P. M. Ferreira, S. Liebler, J. Wittbrodt, Phys. Rev. D **97**, 055008 (2018).
- [22] L. Wang, F. Zhang, X.-F. Han, Phys. Rev. D **95**, 115014 (2017).
- [23] W. Su, M. White, A. G. Williams, Y. Wu, arXiv:1909.09035.
- [24] W. Su, arXiv:1909.09035.
- [25] R. A. Battye, G. D. Brawn, A. Pilaftsis, JHEP **1108**, 020 (2011).
- [26] Heavy Flavor Averaging Group, Eur. Phys. Jour. C **77**, 895 (2017); M. Misiak, M. Steinhauser, Eur. Phys. Jour. C **77**, 201 (2017).
- [27] D. Eriksson, J. Rathsman, O. Stål, Comput. Phys. Commun. **181**, 189 (2010).
- [28] M. Tanabashi et al., [Particle Data Group], Phys. Rev. D **98**, 030001 (2018).
- [29] F. Mahmoudi, Comput. Phys. Commun. **180**, 1579-1673 (2009).
- [30] C. Q. Geng and J. N. Ng, Phys. Rev. D **38**, 2857 (1988) [Erratum-ibid. D **41**, 1715 (1990)].
- [31] H. E. Haber, H. E. Logan, Phys. Rev. D **62**, 015011 (2010).
- [32] G. Degrossi, P. Slavich, Phys. Rev. D **81**, 075001 (2010).
- [33] N. Chen, J. Gu, T. Han, H. Li, Z. Liu, H. Song, S. Su, W. Su, Y. Wu, J. M. Yang, Int. J. Phys. A **34**, 1940012 (2019).
- [34] N. Chen, T. Han, S. Li, S. Su, W. Su, Y. Wu, arXiv:1912.01431.
- [35] J. Bernon, B. Dumont, S. Kraml, Phys. Rev. D **90**, 071301 (2014); S. Kraml, T. Q. Loc, D. T Nhung, L. D. Ninh, arXiv:1908.03952.
- [36] P. Bechtel, O. Brein, S. Heinemeyer, G. Weiglein, K. E. Williams, Comput. Phys. Commun.

- 181**, 138-167 (2010).
- [37] P. Bechtle, O. Brein, S. Heinemeyer, O. Stål, T. Stefaniak, G. Weiglein, K. E. Williams, *Eur. Phys. Jour. C* **74**, 2693 (2014).
- [38] R. V. Harlander, S. Liebler, H. Mantler, *Comput. Phys. Commun.* **184**, 1605 (2013).
- [39] S. Heinemeyer et al. [LHC Higgs Cross Section Working Group Collaboration], arXiv:1307.1347.
- [40] S. Moretti, arXiv:1612.02063.
- [41] ATLAS Collaboration, G. Aad *et al.*, “Search for neutral Higgs bosons of the minimal supersymmetric standard model in pp collisions at  $\sqrt{s} = 8$  TeV with the ATLAS detector,” *JHEP* **11**, 056 (2014).
- [42] CMS Collaboration, “Search for additional neutral Higgs bosons decaying to a pair of tau leptons in  $pp$  collisions at  $\sqrt{s} = 7$  and 8 TeV,” CMS-PAS-HIG-14-029.
- [43] ATLAS Collaboration, “Search for Minimal Supersymmetric Standard Model Higgs Bosons  $H/A$  in the  $\tau\tau$  final state in up to  $13.3 \text{ fb}^{-1}$  of pp collisions at  $\sqrt{s} = 13$  TeV with the ATLAS Detector,” ATLAS-CONF-2016-085.
- [44] CMS Collaboration, “Search for a neutral MSSM Higgs Boson decaying into  $\tau\tau H/A$  with  $12.9 \text{ fb}^{-1}$  of data at  $\sqrt{s} = 13$  TeV,” CMS-PAS-HIG-16-037.
- [45] ATLAS Collaboration, “Search for additional heavy neutral Higgs and gauge bosons in the ditau final state produced in  $36 \text{ fb}^{-1}$  of pp collisions at  $\sqrt{s} = 13$  TeV with the ATLAS detector,” *JHEP* **1801**, 055 (2018).
- [46] CMS Collaboration, “Search for a low-mass pseudoscalar Higgs boson produced in association with a  $b\bar{b}$  pair in pp collisions at  $\sqrt{s} = 8$  TeV,” *Phys. Lett. B* **758**, 296-320 (2016).
- [47] CMS Collaboration, “Search for a light pseudoscalar Higgs boson produced in association with bottom quarks in pp collisions at  $\sqrt{s} = 8$  TeV,” CMS-HIG-15-009.
- [48] ATLAS Collaboration, “Search for scalar diphoton resonances with  $15.4 \text{ fb}^{-1}$  of data collected at  $\sqrt{s} = 13$  TeV in 2015 and 2016 with the ATLAS detector,” ATLAS-CONF-2016-059.
- [49] CMS Collaboration, “Search for resonant production of high mass photon pairs using  $12.9 \text{ fb}^{-1}$  of proton-proton collisions at  $\sqrt{s} = 13$  TeV and combined interpretation of searches at 8 and 13 TeV,” CMS-PAS-EXO-16-027.
- [50] CMS Collaboration, “Search for new resonances in the diphoton final state in the mass range between 70 and 110 GeV in pp collisions at  $\sqrt{s} = 8$  and 13 TeV,” CMS-PAS-HIG-17-013.

- [51] ATLAS Collaboration, G. Aad *et al.*, “Search for a high-mass Higgs boson decaying to a  $W$  boson pair in  $pp$  collisions at  $\sqrt{s} = 8$  TeV with the ATLAS detector,” JHEP **01**, (2016) 032.
- [52] ATLAS collaboration, “Search for a high-mass Higgs boson decaying to a pair of  $W$  bosons in  $pp$  collisions at  $\sqrt{s} = 13$  TeV with the ATLAS detector,” ATLAS-CONF-2016-074.
- [53] ATLAS Collaboration, “Search for diboson resonance production in the  $\ell\nu qq$  final state using  $p$   $p$  collisions at  $\sqrt{s} = 13$  TeV with the ATLAS detector at the LHC,” ATLAS-CONF-2016-062.
- [54] ATLAS Collaboration, “Search for  $WW/WZ$  resonance production in  $\ell\nu qq$  final states in  $pp$  collisions at  $\sqrt{s} = 13$  TeV with the ATLAS detector,” arXiv:1710.07235.
- [55] ATLAS Collaboration, “Search for heavy resonances decaying into  $WW$  in the  $e\nu\mu\nu$  final state in  $pp$  collisions  $\sqrt{s} = 13$  TeV with the ATLAS detector,” Eur. Phys. Jour. C **78**, 24 (2018).
- [56] ATLAS Collaboration, G. Aad *et al.*, “Search for an additional, heavy Higgs boson in the  $H \rightarrow ZZ$  decay channel at  $\sqrt{s} = 8$  TeV in  $pp$  collision data with the ATLAS detector,” Eur. Phys. Jour. C **76**, 45 (2016).
- [57] ATLAS Collaboration, “Search for new phenomena in the  $Z(\rightarrow \ell\ell) + E_{\text{T}}^{\text{miss}}$  final state at  $\sqrt{s} = 13$  TeV with the ATLAS detector,” ATLAS-CONF-2016-056.
- [58] ATLAS Collaboration, “Searches for heavy  $ZZ$  and  $ZW$  resonances in the  $\ell\ell qq$  and  $\nu\nu qq$  final states in  $pp$  collisions at  $\sqrt{s} = 13$  TeV with the ATLAS detector,” ATLAS-CONF-2016-082.
- [59] ATLAS Collaboration, “Study of the Higgs boson properties and search for high-mass scalar resonances in the  $H \rightarrow ZZ^* \rightarrow 4\ell$  decay channel at  $\sqrt{s} = 13$  TeV with the ATLAS detector,” ATLAS-CONF-2016-079.
- [60] ATLAS Collaboration, “Search for heavy  $ZZ$  resonances in the  $\ell^+\ell^-\ell^+\ell^-$  and  $\ell^+\ell^-\nu\nu$  final states using proton proton collisions at  $\sqrt{s} = 13$  TeV with the ATLAS detector,” arXiv:1712.06386.
- [61] ATLAS Collaboration, “Searches for heavy  $ZZ$  and  $ZW$  resonances in the  $\ell\ell qq$  and  $\nu\nu qq$  final states in  $pp$  collisions at  $\sqrt{s} = 13$  TeV with the ATLAS detector,” arXiv:1708.09638.
- [62] CMS Collaboration, V. Khachatryan *et al.*, “Search for two Higgs bosons in final states containing two photons and two bottom quarks,” Phys. Rev. D **94**, 052012 (2016).
- [63] CMS Collaboration, V. Khachatryan *et al.*, “Search for resonant pair production of Higgs bosons decaying to two bottom quark–antiquark pairs in proton–proton collisions at 8 TeV,” Phys. Lett. B **749**, 560-582 (2015).
- [64] CMS Collaboration, V. Khachatryan *et al.*, “Searches for a heavy scalar boson  $H$  decaying to



- a pair of 125 GeV Higgs bosons hh or for a heavy pseudoscalar boson A decaying to Zh, in the final states with  $h \rightarrow \tau\tau$ ,” Phys. Lett. B **755**, 217-244 (2016).
- [65] ATLAS Collaboration, “Search for pair production of Higgs bosons in the  $b\bar{b}b\bar{b}$  final state using proton–proton collisions at  $\sqrt{s} = 13$  TeV with the ATLAS detector,” ATLAS-CONF-2016-049.
- [66] CMS Collaboration, “Search for a massive resonance decaying to a pair of Higgs bosons in the four b quark final state in proton-proton collisions at  $\sqrt{s} = 13$ ,” arXiv:1710.04960.
- [67] CMS Collaboration, “Search for Higgs boson pair production in events with two bottom quarks and two tau leptons in proton-proton collisions at  $\sqrt{s} = 13$ ,” arXiv:1707.02909.
- [68] CMS Collaboration, “Combination of searches for Higgs boson pair production in proton-proton collisions at  $\sqrt{s} = 13$ ,” Phys. Rev. Lett. **122**, 121803 (2019).
- [69] CMS Collaboration, V. Khachatryan *et al.*, “Search for a pseudoscalar boson decaying into a Z boson and the 125 GeV Higgs boson in  $\ell^+\ell^-b\bar{b}$  final states,” Phys. Lett. B **748**, 221-243 (2015).
- [70] ATLAS Collaboration, G. Aad *et al.*, “Search for a CP-odd Higgs boson decaying to Zh in pp collisions at  $\sqrt{s} = 8$  TeV with the ATLAS detector,” Phys. Lett. B **744**, 163-183 (2015).
- [71] ATLAS Collaboration, “Search for heavy resonances decaying into a W or Z boson and a Higgs boson in final states with leptons and b-jets in  $36\text{ fb}^{-1}$  of  $\sqrt{s} = 13$  pp collisions with the ATLAS detector,” arXiv:1712.06518.
- [72] CMS Collaboration, “Search for a heavy pseudoscalar boson decaying to a Z and a Higgs boson at  $\sqrt{s} = 13$  TeV,” Eur. Phys. Jour. C **79**, 564 (2019).
- [73] ATLAS Collaboration, “Search for Higgs bosons decaying to aa in the  $\mu\mu\tau\tau$  final state in pp collisions at  $\sqrt{s} = 8$  TeV with the ATLAS experiment,” Phys. Rev. D **92**, 052002 (2015).
- [74] CMS Collaboration, “Search for light bosons in decays of the 125 GeV Higgs boson in proton-proton collisions at  $\sqrt{s} = 8$  TeV,” JHEP **1710**, 076 (2017).
- [75] CMS Collaboration, “Search for an exotic decay of the Higgs boson to a pair of light pseudoscalars in the final state with two b quarks and two  $\tau$  leptons in proton-proton collisions at  $\sqrt{s} = 13$  TeV,” Phys. Lett. B **785**, 462 (2018).
- [76] CMS Collaboration, “Search for light pseudoscalar boson pairs produced from decays of the 125 GeV Higgs boson in final states with two muons and two nearby tracks in pp collisions at  $\sqrt{s} = 13$  TeV,” arXiv:1907.07235.

- [77] CMS Collaboration, V. Khachatryan *et al.*, “Search for neutral resonances decaying into a Z boson and a pair of b jets or  $\tau$  leptons,” *Phys. Lett. B* **759**, 369-394 (2016).
- [78] CMS Collaboration, A. M. Sirunyan *et al.*, “Search for a heavy pseudoscalar Higgs boson decaying into a 125 GeV Higgs boson and a Z boson in final states with two tau and two light leptons at  $\sqrt{s} = 13$  TeV,” arXiv:1910.11634.